



Published in final edited form as:
Micron. 2002 ; 33(2): 127–132.

Bystander effects caused by nonuniform distributions of DNA-incorporated ^{125}I

Roger W. Howell* and Anupam Bishayee

Division of Radiation Research, Department of Radiology, University of Medicine and Dentistry of New Jersey, New Jersey Medical School, Newark, NJ 07103, USA

Abstract

A three-dimensional tissue culture model was used to investigate the biological effects of nonuniform distributions of DNA-incorporated ^{125}I in mammalian cells. Chinese hamster V79 cells were labeled with ^{125}I -iododeoxyuridine, mixed with unlabeled cells, and multicellular clusters (~ 1.7 mm in diameter) were formed by gentle centrifugation. The highly localized energy deposition caused by ^{125}I decays results in very high equivalent doses delivered to the labeled cells and low equivalent doses delivered to the unlabeled cells. The clusters were assembled and then maintained at 10.5°C for 72 h to allow ^{125}I decays to accumulate, dismantled, and the cells were plated for colony formation. When 100% of the cells were labeled, the survival fraction was exponentially dependent on the mean radioactivity per labeled cell. A two-component exponential response was observed when either 50 or 10% of the cells were labeled. These experimental data, coupled with theoretical dosimetry calculations, indicate that bystander effects play an important role in the killing of unlabeled cells when nonuniform distributions of DNA-incorporated ^{125}I are present.

1. Introduction

Iodine-125 is among the class of radionuclides known as Auger electron emitters. This radionuclide decays by electron capture and internal conversion resulting in the emission of approximately one conversion electron and 25 Auger electrons per decay (Howell, 1992). When localized in the cytoplasm of the cell, ^{125}I results in toxicity typical of radiations of low linear energy transfer (LET). However, when incorporated into DNA in the cell nucleus, ^{125}I is highly radiotoxic (Hofer and Hughes, 1971; Feinendegen, 1975; Hofer et al., 1975; Kassis et al., 1987a,b; Rao et al., 1990). In fact, DNA-incorporated ^{125}I can be as radiotoxic as alpha particles of high LET (Rao et al., 1989; Howell et al., 1991). These and other data are discussed by Sastry (1992) in an in-depth review of the biological effects of ^{125}I . The dosimetric aspects of ^{125}I decay are discussed in depth in a report by Humm et al. (1994).

Recently, there has been a substantial interest in the role of 'bystander effects' in the biological response of mammalian cells to ionizing radiation. It has long been believed that the principal genetic effects of ionizing radiation in mammalian cells are the direct result of DNA damage in irradiated cells that has not been repaired adequately. Therefore, when cells are exposed to radiation, only those cells that receive 'hits' from the emitted radiations would be damaged. No effects would be observed in *bystander* cells that are not 'hit'. Studies from a number of laboratories suggest that these bystander cells do indeed incur significant damage as a consequence of being in the neighborhood of irradiated cells

*Corresponding author: Tel.: +1-973-972-5067, fax: +1-973-972-6474. rhowell@umdnj.edu (R.W. Howell).

(Nagasawa and Little, 1992; Hickman et al., 1994; Deshpande et al., 1996; Lehnert and Goodwin, 1997; Mothersill and Seymour, 1997; Narayanan et al., 1997; Azzam et al., 1998; Bishayee et al., 1999; Nagasawa and Little, 1999; Narayanan et al., 1999; Iyer and Lehnert, 2000a,b; Zhou et al., 2000; Azzam et al., 2001; Bishayee et al., 2001).

The issue of bystander effects is highly relevant to the biological effects of nonuniform distribution of radioactivity. There is evidence of pronounced bystander effects in the form of decreased cell survival when ^3H is localized in the DNA of Chinese hamster lung fibroblast (V79) cells and nonuniformly distributed in multicellular clusters (Bishayee et al., 1999, 2001). Given the highly localized energy deposition associated with ^{125}I decays (Howell, 1992; Sastry, 1992; Humm et al., 1994), it is of interest to examine whether bystander effects can be observed for this prolific Auger electron emitter. In the present communication, the same multicellular cluster model is used to investigate bystander effects caused by nonuniform distributions of ^{125}I .

2. Materials and methods

2.1. Radiochemical and its quantification

$\text{Na } ^{125}\text{I}$ in 0.1 N NaOH (13.6 GBq/ml) was obtained from NEN Life Science Products (Boston, MA). Radiolabeled iododeoxyuridine (^{125}IdU) was synthesized and HPLC purified in our laboratory according to procedures previously reported (Harapanhalli et al., 1994). The ^{125}I activity was quantitated with a Beckman 5500 automatic gamma counter equipped with a 3 inch sodium iodide well crystal (overall counting efficiency = 0.53).

2.2. Cell culture

V79 cells, kindly provided by Dr A. I. Kassis (Harvard Medical School, Boston, MA) were used in the present study, with clonogenic survival serving as the biological endpoint. The cells were cultured in minimum essential medium (MEM) supplemented with 10% heat-inactivated (57°C, 30 min) fetal calf serum, 2 mM L-glutamine, 50 units/ml penicillin, and 50 $\mu\text{g/ml}$ streptomycin (MEMA). The pH of the culture medium was adjusted to 7.0 with NaHCO_3 . All media and supplements used in this study were from Life Technologies (Grand Island, NY). Cells were maintained in Falcon (Becton Dickinson, Lincoln Park, NJ) 175- cm^2 sterile tissue culture flasks at 37°C and 5% CO_2 , 95% air, and subcultured twice weekly or as required (Bishayee et al., 1999). The plating efficiency was about 64%.

2.3. Assembly of multicellular clusters

The protocols are as described earlier (Bishayee et al., 1999). V79 cells growing as monolayers in 175- cm^2 Falcon flasks were washed with 10 ml of phosphate-buffered saline, trypsinized with 0.05% trypsin-0.53 mM EDTA, and suspended at 2×10^6 cells/ml in calcium-free MEM with 10% heat-inactivated (57°C, 30 min) fetal calf serum, 2 mM L-glutamine, 50 units/ml penicillin, and 50 $\mu\text{g/ml}$ streptomycin (MEMB). Aliquots of 1 ml were placed in two sets of sterile 17 \times 100-mm Falcon polypropylene round-bottom culture tubes (10 tubes in each set) and placed on a rocker-roller (Fisher Scientific, Springfield, NJ) for 3–4 h at 37°C in an atmosphere of 95% air and 5% CO_2 . After this conditioning period, 1 ml of MEMB containing various activity concentrations of ^{125}IdU was added to the first set of culture tubes containing 1 ml of V79 cells. The tubes were returned to a rocker-roller at 37°C, 95% air, 5% CO_2 . After 12-h the cells were washed three times with wash MEMA, and resuspended in 2 ml of MEMA, and passed several times through a 21 G needle. Additional tubes containing cells not labeled with radioactivity were identically processed. The radiolabeled cells were then mixed with unlabeled cells to get 100, 50 or 10% radiolabeled cells, pelleted, and transferred directly to a sterile 400- μl polypropylene

microcentrifuge tube (Helena Plastics, San Rafael, CA). The tubes were centrifuged at 1000 rpm for 5 min at 4°C to form clusters with diameter ~ 1.7 mm (4×10^6 cells).

2.4. Cell survival

The microcentrifuge tubes containing the clusters were maintained at 10.5°C for 72 h to allow ^{125}I decay in the absence of cell division. This temperature was selected because V79 cells can remain in the cluster configuration at this temperature for long periods of time (up to 72 h) without decrease in plating efficiency. This was also true for V79 cells in suspension culture (Bishayee et al., 2001). The supernatant was then carefully removed and the tubes were vortexed to disperse the cell clusters. The cells were washed three times with 10 ml of wash MEMA, resuspended in 2 ml of wash MEMA, passed several times through a 21 G needle (resulting in a single cell suspension with a doublet frequency of only 2.4%), serially diluted, seeded in triplicate into 60×15 mm Falcon tissue culture dishes, and incubated at 37°C with 95% air and 5% CO_2 . Between 200 and 20,000 cells were seeded into each dish depending on the amount of ^{125}IdU used. Aliquots were taken from each tube before serial dilution as above and the mean radioactivity per cell was determined. After seven days, the surviving fraction compared to controls was determined.

3. Discussion

3.1. 100% labeling: response of multicellular clusters and cell suspensions

Fig. 1 illustrates the surviving fraction of cells maintained in multicellular clusters for 72 h as a function of ^{125}I activity (mBq) per labeled cell. Also shown is the survival curve obtained when cells were identically prepared except maintained as a single-cell suspension for 72 h at 10.5°C. In this case, radiolabeled cells were suspended in 2 ml MEMB and placed on the rocker roller for 72 h at 10.5°C (see Bishayee et al., 2000, for experimental details). As expected for 100% labeling with ^{125}IdU (Howell et al., 1991; Bishayee et al., 2000), the response is monoexponential. The data were fitted by least squares to the relationship,

$$\text{SF} = (1 - b)e^{-A/A_1} + be^{-A/A_2} \quad (1)$$

where SF is the surviving fraction, A is the activity per labeled cell and b , A_1 and A_2 are the fitted parameters. The parameters A_1 and A_2 are analogous to D_0 values for the first and second components, respectively. With $b = 0$ for monoexponential response, the fitted values of A_1 for cluster and suspension are 0.48 ± 0.05 and 0.52 ± 0.02 mBq/cell, respectively. The response of the cells to incorporated ^{125}IdU is essentially the same whether the cells are arranged in the form of a cluster or maintained as a single-cell suspension. Therefore, this suggests that the cross-dose received by the cells in the 100% labeling case is not biologically significant.

It is of interest to point out that the A_1 value for cell suspension is not in good agreement with our published value of 0.15 mBq/cell (Bishayee et al., 2000). In these earlier studies, all procedures were identical except that cells were rolled at a concentration of only $2 \times 10^5/\text{ml}$ as opposed to the present value of $2 \times 10^6/\text{ml}$. The large number of cells required for the present experiments led us to grow the cells in large 175 cm^2 flasks, and, rather than using a low-density of cells in exponential growth, cells were allowed to achieve 80–90% confluency prior to harvesting. This had a significant impact on the cell cycle status of the cells as evidenced by standard propidium iodide flow cytometry analysis. Specifically, cell cycle analysis after harvesting of low-density cells from 175 cm^2 flasks revealed the

following distribution: G₁ 54%, G₂ 8%, S 38%. The same distribution was observed after this population was suspended in MEMB and placed on the rocker roller for 12 h (time during which cells were labeled with the radiochemical). In contrast, high-density cells exhibited the following distribution after harvesting: G₁ 76%, G₂ 5%, S 19%. After the 12 h rolling period in the presence of ¹²⁵IIdU, the distribution was: G₁ 49%, G₂ 9%, S 42%. Hofer et al. (1992) showed that DNA-incorporated ¹²⁵I was highly toxic (akin to high-LET alpha particles) in Chinese hamster ovary (CHO) cells when the cells were pulse labeled in early-S, allowed to progress to late-S/G₂ phase, and then frozen for decay accumulation. They were far less toxic (akin to low-LET X-rays) when they were pulse labeled in early-S phase and frozen in early-S phase for decay accumulation. The cell cycle distribution for our confluent culture shows a large percent of the population was synchronized in G₁ upon harvesting, and then released upon transferring to suspension culture for labeling. The distribution after the 12 h labeling period shows that there was a large shift from G₁-phase into S-phase and only a small shift from S into G₂. Given that the number of the cells in the population did not change appreciably during this labeling period, few cells in the population moved through M-phase. The differences in cell cycle distribution between the high- and low-density harvested cells had a significant impact on the distribution of phases when the cells were at 10.5°C for decay accumulation, and may have a significant impact on the period in S-phase during which the cells were labeled. This may provide an explanation for the departure of the present value of A₁ for suspended cells compared to our previous value. Detailed cell cycle analyses at various times throughout the experiment are required to confirm and refine this hypothesis.

3.2. 100, 50 and 10% labeling: response of multicellular clusters

Fig. 2 shows the cell survival fraction as a function of radioactivity per labeled cell for multicellular clusters wherein 100, 50 or 10% of the cells were labeled with ¹²⁵IIdU. The data for 100% labeling includes data from Fig. 1 as well as data from two additional experiments. A least squares fit to the combined data (four experiments) gives A₁ (100%) = 0.41 ± 0.02 mBq/cell. Two-component exponential survival curves emerge when 50% and 10% of the cells in the cluster are labeled (Fig. 2 inset). In the 50% labeling case, as the activity per labeled cell increases, the survival fraction drops sharply to about 50% and then continues to drop albeit with a shallower slope. The first component of the two-component survival curve indicates lethality to the radiolabeled cells whereas the second component represents killing of unlabeled cells. A similar pattern emerges for 10% labeling, however, the initial drop ends at about 90% survival. These data are fitted to two-component exponential functions as defined by Eq. (1). Table 1 summarizes the fitted parameters for the different labeling conditions.

3.3. Absorbed dose to labeled and unlabeled cells

The radionuclide ¹²⁵I emits short-range conversion electrons and Auger electrons with ranges in water from 0 to 20 μm (Howell, 1992). Because the ¹²⁵IIdU is localized in the cell nucleus, the extremely short-range Auger electrons only irradiate the cells containing radioactivity. However, the conversion electrons and K-shell Auger electrons are sufficiently energetic to cross-irradiate the unlabeled cells. Therefore, the absorbed dose must be calculated for both the labeled and unlabeled cells. The mean diameter of a V79 cell is 10 μm and its nucleus has a mean diameter of 8 μm (Howell et al., 1991). A spherical cluster of 4 × 10⁶ cells in hexagonal close packed geometry is about 1750 μm in diameter. Using the model of Goddu et al. (1994) and the ¹²⁵I radiation spectrum (Howell, 1992), the mean self absorbed dose to the nucleus of a labeled cell per unit cumulated activity in the nucleus of the labeled cell is S_{self}(labeled ← labeled) = 6.60 × 10⁻³ Gy/Bq s. The mean self absorbed dose to the nucleus D_{self}(labeled) = \tilde{A} S_{self}(labeled ← labeled) = 2.25 Gy per mBq in the cell. The mean cross-dose to the unlabeled cell depends on the percentage of cells in

the cluster that are labeled. The mean cross-doses D_{cross} to the nucleus of the cells in the 1750 μm cluster are 0.055, 0.27, and 0.55 Gy per mBq in the labeled cell for 10, 50 and 100% labeling cases, respectively. The cross-doses are essentially the same for the labeled and unlabeled cells.

3.4. Evidence of bystander effects in the unlabeled cells

Now that the cross-doses have been calculated, one can examine the presence of bystander effects imparted to the unlabeled cells. In published studies (Bishayee et al., 1999), the response of the cluster to chronic external irradiation with ^{137}Cs gamma rays delivered under identical conditions was linear-quadratic (LQ) ($S = \exp(-\alpha D - \beta D^2)$) with $\alpha = 0.044 \text{ Gy}^{-1}$ and $\beta = 0.00391 \text{ Gy}^{-2}$. This corresponds to a D_{37} of 11.3 Gy. Assuming that the ^{125}I conversion electrons and K-shell Auger electrons (energies ranging from 20 to 30 keV) induce a linear-quadratic response that is the same as chronic external gamma rays, one can project the survival fraction of the unlabeled cells. Consider the case of 10% labeling case where 250 mBq/labeled cell is required to achieve an overall survival fraction for the mixed population of 0.001. In this case, $D_{\text{unlabeled}} = D_{\text{cross}} = 250 \text{ mBq} (0.055 \text{ Gy/mBq}) = 13.8 \text{ Gy}$. Using the LQ model above, the surviving fraction of unlabeled cells should be about 0.26. Given that essentially none of the labeled cells will survive 250 mBq, the overall survival fraction for the population is expected to be 0.13. This is far greater than the experimentally observed value of 0.001. Similar results emerge in the 50% labeling case. This suggests that bystander effects are operational when nonuniform distributions of ^{125}I are present. Furthermore, bystander effects in unlabeled cells far outweigh the effects of the cross-irradiation.

3.5. Equivalent dose to the labeled and unlabeled cells

The importance of bystander effects in unlabeled cells caused by nonuniform distributions can be better understood by a more detailed dosimetric analysis. Although the absorbed dose is a useful quantity, the biological effectiveness of the self- and cross-doses are very different for DNA-incorporated ^{125}I IdU. The relative biological effectiveness of the self-dose for ^{125}I IdU can be obtained for this model by comparison with the response of the cluster to chronic external irradiation with ^{137}Cs gamma rays delivered under identical conditions. As noted in the previous subsection, the chronic gamma dose required to achieve 37% survival (D_{37}) is 11.3 Gy. For 100% labeling, the total mean D_{37} is the sum of the self and cross-doses: $D_{37}(^{125}\text{I}IdU) = D_{\text{self}} + D_{\text{cross}} = 0.41 \text{ mBq} (2.25 \text{ Gy/mBq} + 0.55 \text{ Gy/mBq}) = 1.15 \text{ Gy}$. The relative biological effectiveness (RBE) of the mixed radiation field at 37% survival is therefore $\text{RBE}_{\text{mixed}} = D_{37}(\text{gamma})/D_{37}(^{125}\text{I}IdU) = 11.3/1.15 = 9.8$. The RBE of the mixed radiation field can be expressed as a weighted sum

$$\text{RBE}_{\text{mixed}} = q_{\text{self}} \text{RBE}_{\text{self}} + q_{\text{cross}} \text{RBE}_{\text{cross}}, \quad (2)$$

where q_{self} and q_{cross} represent the fraction of the total dose delivered by the self- and cross-doses, respectively, and RBE_{self} and $\text{RBE}_{\text{cross}}$ represent the RBE of the self- and cross-doses, respectively (Azure et al., 1994). Assuming that the RBE for the cross-dose is equivalent to that for chronic external ^{137}Cs gamma rays, then $\text{RBE}_{\text{cross}} = 1$. Solving Eq. (2) for RBE_{self} , one obtains $\text{RBE}_{\text{self}} = 12$. This high RBE value is in keeping with the high RBE values that have been observed for ^{125}I IdU.

Given the different RBE's for the self- and cross-doses, one cannot directly compare the dose to the labeled cells with the dose to the unlabeled cells in 10 and 50% labeling cases. To accomplish this, one can invoke the equivalent dose defined as $H = \sum w_R D_R$ where w_R is

the radiation weighting factor and the sum is over R different contributions to the total radiation dose (ICRP, 1991). With $w_R = \text{RBE}_R$, then the equivalent dose to the cells for

$$H_{\text{labeled}} = \text{RBE}_{\text{cross}} D_{\text{cross}} + \text{RBE}_{\text{self}} D_{\text{self}}, \quad (3)$$

The equivalent dose to the unlabeled cells is simply given by

$$H_{\text{unlabeled}} = \text{RBE}_{\text{cross}} D_{\text{cross}}, \quad (4)$$

Finally, the ratio of the equivalent dose to the labeled cells relative to the unlabeled cells is obtained by dividing Eq. (3) by Eq. (4).

$$f = \frac{H_{\text{labeled}}}{H_{\text{unlabeled}}} = 1 + \frac{\text{RBE}_{\text{self}} D_{\text{self}}}{\text{RBE}_{\text{cross}} D_{\text{cross}}} \quad (5)$$

For 10% labeling, $\text{RBE}_{\text{self}}/\text{RBE}_{\text{cross}} = 12$, $D_{\text{self}}/D_{\text{cross}} = 2.25/0.055 = 41$, and $f_{10\%} = 490$. For 50% labeling, $\text{RBE}_{\text{self}}/\text{RBE}_{\text{cross}} = 12$, $D_{\text{self}}/D_{\text{cross}} = 2.25/0.27 = 8.3$, and $f_{50\%} = 100$. Therefore, the equivalent dose to the labeled cells is 490 and 100 times greater than the equivalent dose to the unlabeled cells when 10 and 50% of the cells are labeled, respectively. These values are helpful in terms of understanding the relative unimportance of the cross-dose in the overall response of the mixed cell population. In fact, these values are similar to those determined earlier for ^3H -thymidine where marked bystander effects were also observed (Bishayee et al., 2001).

In conclusion, the present study provides new data on the biological effects of nonuniform distributions of incorporated radioactivity using a novel approach to specifically control the degree of nonuniformity. Specifically, this study establishes the response of V79 multicellular clusters to DNA-incorporated ^{125}I and furnishes additional evidence that bystander effects play a significant role in determining the biological effects of tissue-incorporated radioactivity.

Acknowledgments

The authors greatly appreciate the insightful comments and suggestions provided by Edouard I. Azzam and Sonia M. de Toledo, Department of Radiology, UMDNJ, New Jersey Medical School. We are also thankful to Dana Stein for technical assistance with the flow cytometry and Thomas N. Denny for providing access to the flow cytometer. This work was supported in part by USPHS Grant Nos. R01 CA83838 (RWH) and shared instrumentation grant 1 S10 RR14753-01 (TND).

References

- Azure MT, Archer RD, Sastry KSR, Rao DV, Howell RW. Biologic effect of ^{212}Pb localized in the nucleus of mammalian cells: role of recoil energy in the radiotoxicity of internal alpha emitters. *Radiat Res* 1994;140:276–283. [PubMed: 7938477]
- Azzam EI, de Toledo SM, Gooding T, Little JB. Intercellular communication is involved in the bystander regulation of gene expression in human cells exposed to very low fluences of alpha particles. *Radiat Res* 1998;150:497–504. [PubMed: 9806590]
- Azzam EI, de Toledo SM, Little JB. Direct evidence for the participation of Gap-Junction mediated Intercellular Communication in the transmission of damage signals from alpha-particle irradiated to non-irradiated cells. *Proc Natl Acad Sci USA* 2001;98:473–478. [PubMed: 11149936]

- Bishayee A, Rao DV, Howell RW. Evidence for pronounced bystander effects caused by nonuniform distributions of radioactivity using a novel three-dimensional tissue culture model. *Radiat Res* 1999;152:88–97. [PubMed: 10428683]
- Bishayee A, Rao DV, Bouchet LG, Bolch WE, Howell RW. Radioprotection by DMSO against cell death caused by intracellularly localized I-125, I-131, and Po-210. *Radiat Res* 2000;153:416–427. [PubMed: 10761002]
- Bishayee A, Hill HZ, Stein D, Rao DV, Howell RW. Free-radical initiated and gap junction-mediated bystander effect due to nonuniform distribution of incorporated radioactivity in a three-dimensional tissue culture model. *Radiat Res* 2001;155:335–344. [PubMed: 11175669]
- Deshpande A, Goodwin EH, Bailey SM, Marrone BL, Lehnert BE. Alpha-particle-induced sister chromatid exchange in normal human lung fibroblasts—evidence for an extranuclear target. *Radiat Res* 1996;145:260–267. [PubMed: 8927692]
- Feinendegen LE. Biological damage from the Auger effect, possible benefits. *Radiat Environ Biophys* 1975;12:85–99. [PubMed: 1101289]
- Goddu SM, Rao DV, Howell RW. Multicellular dosimetry for micrometastases: Dependence of self-dose versus cross-dose to cell nuclei on type and energy of radiation and subcellular distribution of radionuclides. *J Nucl Med* 1994;35:521–530. [PubMed: 8113908]
- Harapanhalli RS, Narra VR, Yaghmai V, Azure MT, Goddu SM, Howell RW, Rao DV. Vitamins as radioprotectors in vivo II. Protection by vitamin A and soybean oil against radiation damage caused by internal radionuclides. *Radiat Res* 1994;139:115–122. [PubMed: 8016300]
- Hickman AW, Jaramillo RJ, Lechner JF, Johnson NF. Alpha-particle-induced p53 protein expression in a rat lung epithelial cell strain. *Cancer Res* 1994;54:5797–5800. [PubMed: 7954402]
- Hofer KG, Hughes WL. Radiotoxicity of intranuclear tritium, iodine-125 and iodine-131. *Radiat Res* 1971;47:94–109. [PubMed: 5559387]
- Hofer KG, Harris CR, Smith JM. Radiotoxicity of intracellular Ga-67, I-125, H-3. Nuclear versus cytoplasmic radiation effects in murine L1210 leukaemia. *Int J Radiat Biol* 1975;28:225–241.
- Hofer, KG.; Van Loon, N.; Schneiderman, MH.; Charlton, DE. High and low-LET cytotoxic effects of DNA-associated iodine-125. In: Howell, RW.; Narra, VR.; Sastry, KSR.; Rao, DV., editors. *Biophysical Aspects of Auger Processes*. American Institute of Physics; Woodbury, NY: 1992. p. 227-248.
- Howell RW. Radiation spectra for Auger-electron emitting radionuclides: Report No. 2 of AAPM Nuclear Medicine Task Group No. 6. *Med Phys* 1992;19:1371–1383. [PubMed: 1461199]
- Howell RW, Rao DV, Hou D-Y, Narra VR, Sastry KSR. The question of relative biological effectiveness and quality factor for Auger emitters incorporated into proliferating mammalian cells. *Radiat Res* 1991;128:282–292. [PubMed: 1961925]
- Humm JL, Howell RW, Rao DV. Dosimetry of Auger electron emitting radionuclides: Report No. 3 of the AAPM Nuclear Medicine Task Group No. 6. *Med Phys* 1994;21:1901–1901. [PubMed: 7700197]
- ICRP. International Commission on Radiological Protection. Pergamon; Oxford: 1991. Publication 60. 1990 Recommendations.
- Iyer R, Lehnert BE. Factors underlying the cell growth-related bystander responses to alpha particles. *Cancer Res* 2000a;60:1290–1298. [PubMed: 10728689]
- Iyer R, Lehnert BE. Minireview: effects of ionizing radiation in targeted and nontargeted cells. *Arch Biochem Biophys* 2000b;376:14–25. [PubMed: 10729186]
- Kassis AI, Fayad F, Kinsey BM, Sastry KSR, Taube RA, Adelstein SJ. Radiotoxicity of I-125 in mammalian cells. *Radiat Res* 1987a;111:305–318. [PubMed: 3628718]
- Kassis AI, Sastry KSR, Adelstein SJ. Kinetics of uptake, retention, and radiotoxicity of ¹²⁵IuDR in mammalian cells: Implications of localized energy deposition by Auger processes. *Radiat Res* 1987b;109:78–89. [PubMed: 3809393]
- Lehnert BE, Goodwin EH. Extracellular factor(s) following exposure to alpha particles can cause sister chromatid exchanges in normal human cells. *Cancer Res* 1997;57:2164–2171. [PubMed: 9187116]
- Mothersill C, Seymour C. Medium from irradiated human epithelial cells but not human fibroblasts reduces the clonogenic survival of unirradiated cells. *Int J Radiat Biol* 1997;71:421–427. [PubMed: 9154145]

- Nagasawa H, Little JB. Induction of sister chromatid exchanges by extremely low doses of alpha-particles. *Cancer Res* 1992;52:6394–6396. [PubMed: 1423287]
- Nagasawa H, Little JB. Unexpected sensitivity to the induction of mutations by very low doses of alpha-particle irradiation: evidence for a bystander effect. *Radiat Res* 1999;152:552–557. [PubMed: 10521933]
- Narayanan PK, Goodwin EH, Lehnert BE. Alpha particles initiate biological production of superoxide anions and hydrogen peroxide in human cells. *Cancer Res* 1997;57:3963–3971. [PubMed: 9307280]
- Narayanan PK, LaRue KEA, Goodwin EH, Lehnert BE. Alpha particles induce the production of interleukin-8 by human cells. *Radiat Res* 1999;152:57–63. [PubMed: 10381841]
- Rao DV, Narra VR, Howell RW, Govelitz GF, Sastry KSR. In-vivo radiotoxicity of DNA-incorporated I-125 compared with that of densely ionising alpha-particles. *Lancet* 1989;II:650–653. [PubMed: 2570902]
- Rao DV, Narra VR, Howell RW, Sastry KSR. Biological consequence of nuclear versus cytoplasmic decays of I-125: Cysteamine as a radioprotector against Auger cascades in vivo. *Radiat Res* 1990;124:188–193. [PubMed: 2247599]
- Sastry KSR. Biological effects of the Auger emitter ¹²⁵I: A review. Report No. 1 of AAPM Nuclear Medicine Task Group No. 6. *Med Phys* 1992;19:1361–1370. [PubMed: 1461198]
- Zhou H, Randers-Pehrson G, Waldren CA, Vannais D, Hall EJ, Hei TK. Induction of a bystander mutagenic effect of alpha particles in mammalian cells. *Proc Natl Acad Sci USA* 2000;97:2099–2104. [PubMed: 10681418]

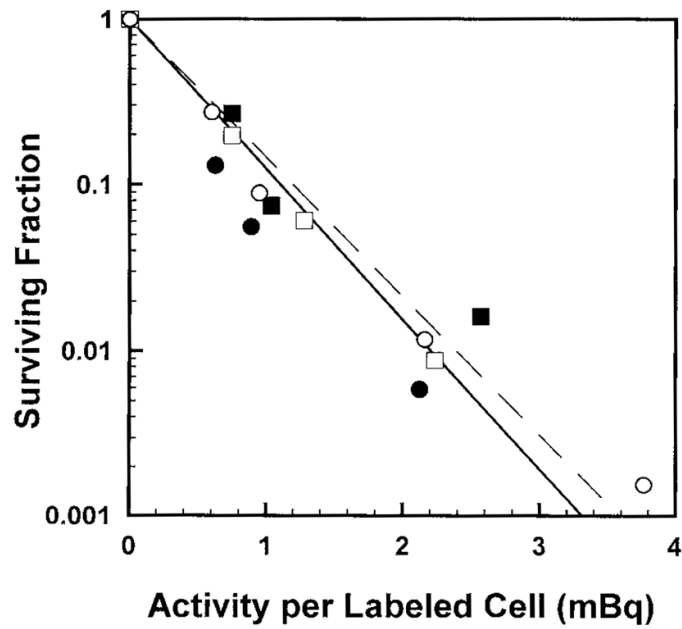


Fig. 1. Survival of V79 cells as a function of activity per labeled cell wherein 100% of the cell population was labeled with ^{125}I dU. Cells were maintained in MEMA as multicellular clusters (\bullet , \blacksquare) or as suspensions (\circ , \square). Circles and squares represent independent experiments.

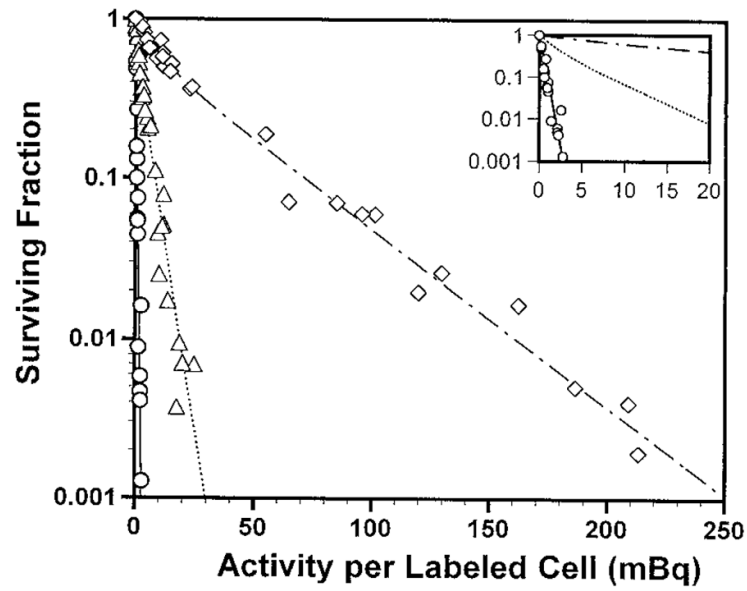


Fig. 2. Survival of V79 cells as a function of activity per labeled cell wherein 100% (\circ), 50% (Δ), or 10% (\diamond) of the cells were labeled with ^{125}I dU and used to form multicellular clusters. Data from four, six, and four independent experiments are presented for each case, respectively. Standard errors for each data point are of the order of the dimensions of the symbols. The inset is an enlargement of the low activity per labeled cell region.

Table 1

Fitted parameters for survival curves for multicellular clusters

Treatment	% cells labeled	No. of experiments	b	A_1^a (mBq/labeled cell)	A_2^a (mBq/labeled cell)
$^{125}\text{I}dU$	100	4	0	0.41 ± 0.02^b	–
$^{125}\text{I}dU$	50	6	0.55 ± 0.08	1.6 ± 0.3	4.7 ± 0.5
$^{125}\text{I}dU$	10	4	0.61 ± 0.08	9.2 ± 2.6	39.2 ± 1.6

^a A_1 and A_2 are analogous to the D_0 's of the first (labeled cells) and second (by stander cells) components of the fitted survival curve (Eq. (1)).^b SEM.